Actuation Model for Lamb Wave Excitation in Composite Plates Using Piezoelectric-Flexoelectric Actuators

SURAJ KUMAR ROUT and SANTOSH KAPURIA

ABSTRACT

Among various SHM techniques, guide-wave-based methods are mostly explored for their effectiveness in damage detection. However, despite the growing interest in this area, no analytical models have been developed to date for the actuation of Lamb waves in composite structures using piezoelectric and flexoelectric transducers. This article develops a theoretical model for actuation of composite plates using physically modeled adhesively bonded piezoelectric-flexoelectric transducers. The model incorporates both interfacial shear and peel stresses at the interface of the actuator and host composite laminate. The tractions induced by the actuator onto the plate surface are determined by modeling the actuator and the laminated plate as Mindlin plates. The formulation results in a seventh-order differential equation for the interfacial shear stress, which is solved in closed form by satisfying stress-free boundary conditions at the actuator and plate edges. The peel stress is subsequently determined from the differential relation in terms of the interfacial shear stress. For validation, the longitudinal distributions of interfacial shear and peel stresses are compared with the ABAQUS' continuum-based finite element results. A comprehensive numerical study has been performed to demonstrate the effect of adhesive and host laminate thickness on the distributions of interfacial shear stress and its peak amplitude.

INTRODUCTION

Due to the exceptional properties of fiber-reinforced composite materials, including high specific strength, stiffness, and resistance to fatigue and corrosion, they are highly desirable for various high-performance applications, such as biomedical devices, aircraft, spacecraft, automobiles, marine vessels, turbine blades, and sports equipment. However, their inherently anisotropic and inhomogeneous nature makes them vulnerable to sub-surface delamination, which can lead to catastrophic failure of structures. To ensure the safety and reliability of composite structures, detecting delamination early through a real-time damage detection technique using inbuilt transducers known as structural health monitoring (SHM) is essential.

Lamb waves are widely used as guided waves in SHM applications for real-time damage detection. Most such SHM applications employ surface-bonded or embedded piezoelectric wafer active sensors (PWAS) as transducers due to their low cost, small size, high range of linearity, and unobtrusive nature. Piezoelectric materials generate electric fields from induced strain (direct piezoelectric effect) and induce mechanical

Suraj Kumar Rout, PhD Student, Email: suraj.kumar.rout6696@gmail.com. Department of Applied Mechanics, Indian Institute of Technology Delhi, New Delhi 110016, India

Santosh Kapuria, Professor, Email: kapuria@am.iitd.ac.in; Tel. +91-11-26591218. Department of Applied Mechanics, Indian Institute of Technology Delhi, New Delhi 110016, India

deformation by applying electric potential (converse piezoelectric effect). In recent years, a relatively novel electromechanical phenomenon known as flexoelectricity has attracted enormous attention as a potential alternative to piezoelectric materials for actuation, sensing, and energy harvesting applications. The flexoelectric effect describes the generation of electric polarisation charges on the surfaces due to the non-uniform strain field (direct flexoelectric effect) and mechanical strain caused by the applied electric field gradient (converse flexoelectric effect) [1].

The excitation of guided Lamb waves by these transducers heavily depends on their dimensions, material properties, and bonding layer, which must be carefully studied for damage detection. To achieve this, accurate closed-form analytical solutions are required for Lamb wave actuation and sensing in host structures using surface-bonded electromechanical transducers. While such analytical models have been successfully developed for isotropic substrates employing surface-bonded piezoelectric transducers [2, 3], there is currently no available literature addressing actuation and sensing in composite laminate host structures using surface-bonded piezoelectric or flexoelectric transducers.

In this article, a mathematical model has been developed for actuation of a composite host laminate using an adhesively bonded piezoelectric-flexoelectric transducer on the top surface of the host plate. The model incorporates both shear and normal deformation compliances in the bonding layer for the stress transfer between the actuator and the host laminated composite plate. Both the actuator and the host plate are modeled using the Reissner-Mindlin plate theory. A seventh-order differential equation is obtained for interfacial shear stress, which is solved by satisfying stress-free boundary conditions at the actuator and plate edges. Subsequently, the expression for interfacial peel stress is obtained through a differential relation with shear stress. For the verification of the present analytical model, the longitudinal distributions of shear and peel stresses are compared with the 2D FE solution. A numerical study has been presented to show the effect of adhesive thickness on the distribution of interfacial shear stress. Furthermore, the influence of both adhesive and host plate thickness on the peak magnitude of the interfacial shear stress is investigated.

ACTUATOR MODEL

In this section, we focus on developing a theoretical actuation model for a flexoelectric-piezoelectric transducer, which is adhesively bonded to the top surface of a composite laminate host structure. All the dimensions of transducer-adhesive-substrate system are depicted in Fig. 1. The composite laminate consists of L number of perfectly bonded laminae. Each lamina is made of unidirectional fiber-reinforced composite material exhibiting orthotropic material symmetry. The count of the number of lamina starts from the bottom, and $z = z_0$ denotes the bottom surface of the first lamina. z_k corresponds to the top surface of the kth lamina with k ranging from 1 to L as shown in Fig. 1. The plane $z = 0$ passes either through the bottom of the k_0th layer or through the middle of it and the z- axis passes through the thickness of the laminate (Fig. 1). Similarly, the transducer's corresponding longitudinal and transverse axes are presented in Fig. 1.

We assume that the actuator and composite laminate have infinite width in transverse in-plane direction, and consequently the strain components on the y-plane vanish, $\varepsilon_y = \gamma_{yx} = \gamma_{yz} = 0$. Following most laminate theories, we assume $\sigma_z \simeq 0$. The actuator

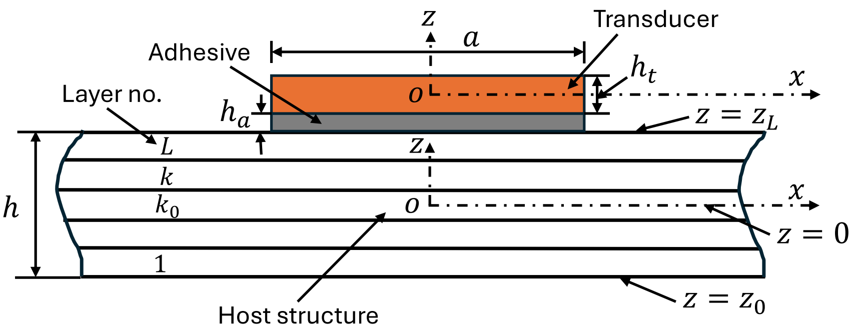

Figure 1. Host laminated composite plate bonded to flexoelectric-piezoelectric transducer through an adhesive layer

is actuated by applying uniform potential ϕ at the top surface of the transducer and we assume E_z be the only dominant electric field component, with gradients $E_{z,x} = E_{z,y} = 0$. Electric field is defined in terms of the electric potential ϕ as $E_i = -\phi_{,i}$. Based on the aformentioned assumptions, for a class mm2 symmetry orthorhombic piezoelectric-flexoelectric dielectric material, the strain components can be related to the stress components as [4]

$$\varepsilon_x = \bar{s}_{11}\sigma_x^p + \bar{d}_{31}E_z - \bar{\lambda}_{19}E_{z,z}, \qquad \gamma_{xz} = \frac{s_{55}}{k_x}\tau_{xz}^p, \tag{1}$$

where superscript p corresponds to physical stress and for elastic solid it is Cauchy stress. k_x is the shear correction factor. $\bar{s}_{11}$, $\bar{d}_{31}$, and $\bar{\lambda}_{19}$ denote the effective elastic compliance, piezoelectric strain, and flexoelectric constants, respectively.

Similar to the actuator, the constitutive relation for the composite laminate host structure under plane strain conditions can be presented as [5]

$$\sigma_x = \hat{Q}_{11}\varepsilon_x, \qquad \tau_{xz} = k_x\hat{Q}_{55}\gamma_{xz}, \tag{2}$$

where $\hat{Q}_{11}$ and $\hat{Q}_{55}$ denote the reduced stiffness coefficients.

In this model, infinite width panel is considered as cross-ply laminate. We model both the actuator and host laminate using the first order shear deformation theory (FSDT). Accordingly, the in-plane displacement at the top surface of the host laminate (u_1) and bottom surface of the actuator (u_2) can be expressed as

$$u_2(x,z) = u_{0_t}(x) - \frac{h_t}{2}[\psi_t(x) - w_{t,x}(x)], \quad u_1(x,z) = u_{0_s}(x) + \frac{h}{2}[\psi_s(x) - w_{s,x}(x)]. \tag{3}$$

where u_0 and w denote the mid-surface displacements along x and z direction and ψ is the shear rotation. The subscripts (or superscripts used subsequently) s and t denote the variables associated with the host structure and the transducer, respectively.

Under the plane strain conditions and zero body forces, the static equilibrium equations for the actuation region ($-a/2 \leq x \leq a/2$) can be obtained as [4]

$$N_{x,x}^t - \tau = 0, \qquad M_{x,x}^t + \frac{h_t}{2}\tau - Q_x^t = 0, \qquad Q_{x,x}^t - \sigma_z = 0, \tag{4}$$

$$N_{x,x}^s + \tau = 0, \qquad M_{x,x}^s + \frac{h}{2}\tau - Q_x^s = 0, \qquad Q_{x,x}^s + \sigma_z = 0, \tag{5}$$

where N_x^k, M_x^k, and Q_x^k $(k = s, t)$ are the in-plane stress, moment, and transverse shear stress resultants, respectively, defined as

$$N_x^k = \int_z \sigma_x^k \mathrm{d}z, \qquad M_x^k = \int_z \sigma_x^k z \mathrm{d}z, \qquad Q_x^k = \int_z \tau_{xz}^k \mathrm{d}z. \tag{6}$$

The constitutive relations for the thin adhesive layer, defined by interfacial shear stress τ and peel stress σ_z, can be expressed as

$$\tau = G_a \gamma_a = \left(\frac{u_2 - u_1}{\beta_1}\right), \qquad \sigma_z = E_a \varepsilon_z = \left(\frac{w_t - w_s}{\beta_2}\right), \tag{7}$$

where $\beta_1 = h_a/G_a$ and $\beta_2 = h_a/E_a$. G_a and E_a are the shear and Young's moduli of the adhesive layer, respectively. By differentiating Eqs. $(7)_1$ and $(7)_2$ three and four times, respectively, with respect to x and employing Eqs. (3)-(6), we get two coupled ordinary differential equations (ODEs) in terms of τ and σ_z as

$$\tau_{,xxx} = \Gamma_{11}\tau_{,x} - \Gamma_{12}\sigma_z, \tag{8}$$

$$\sigma_{z,xxxx} = \Gamma_{21}\tau_{,x} - \Gamma_{22}\sigma_z + \hat{S}_{55}\sigma_{z,xx}, \tag{9}$$

where Γ_{11}, Γ_{12}, Γ_{21}, Γ_{22}, and $\hat{S}_{55}$ are the constants involving the geometry and material properties of the host laminate-adhesive-actuator system. The method of substitution is applied to get an uncoupled ODE for τ as

$$\tau_{,xxxxxxx} - \hat{\Gamma}_{11}\tau_{,xxxxx} + \hat{\Gamma}_{22}\tau_{,xxx} - \Gamma\tau_{,x} = 0, \tag{10}$$

where

$$\hat{\Gamma}_{11} = \Gamma_{11} + \hat{S}_{55}, \qquad \hat{\Gamma}_{22} = \Gamma_{22} + \Gamma_{11}\hat{S}_{55}, \qquad \Gamma = (\Gamma_{11}\Gamma_{22} - \frac{\beta_1}{\beta_2}\Gamma_{12}^2). \tag{11}$$

The general solution of τ is derived by solving seventh-order homogeneous ODE (Eq. (10)). By taking $\tau = Ae^{\lambda x}$ as a solution of Eq. (10) and employing Cardano's method [6] for $G > 0$, as followed in our recent publication [4], we obtain the seven roots in the following form:

$$\begin{array}{l} \lambda_0 = 0, \quad \lambda_1 = p, \quad \lambda_2 = -p, \quad \lambda_3 = \alpha + i\gamma, \\ \lambda_4 = \alpha - i\gamma, \quad \lambda_5 = -\alpha + i\gamma \quad \lambda_6 = -\alpha - i\gamma. \end{array} \tag{12}$$

Since the loading, geometry, and boundary conditions are symmetric about $x = 0$, the general solution of τ can be expressed by retaining only the antisymmetric part as

$$\tau(x) = C_1 \sinh(px) + C_3 \sinh(\alpha x)\cos(\gamma x) + C_5 \cosh(\alpha x)\sin(\gamma x). \tag{13}$$

where C_i are arbitrary constants, obtained by imposing appropriate boundary conditions given below

$$N_x^t|_{x=a/2} = 0, \qquad M_x^t|_{x=a/2} = 0, \qquad Q_x^t|_{x=a/2} = 0, \tag{14}$$

$$N_x^s|_{x=a/2} = 0, \qquad M_x^s|_{x=a/2} = 0, \qquad Q_x^s|_{x=a/2} = 0. \tag{15}$$

Using Eqs. (14) and (15), we obtain three boundary conditions in terms of τ and σ_z as

$$\text{For } x = a/2: \ \tau_{,x} = \frac{1}{\beta_1}\left[\bar{d}_{31}E_z - \frac{6\bar{\lambda}_{19}}{h_t}\bar{E}_z\right], \ \sigma_{z,xx} = -\frac{12\bar{\lambda}_{19}}{h_t^2\beta_2}\bar{E}_z, \ \sigma_{z,xxx} - \Gamma_{21}\tau = 0. \tag{16}$$

where $\bar{E}_z$ denotes the average value of E_z along the thickness of thin actuator, which too can be taken as $E_z(= -\phi/h_t)$. The expression for σ_z in terms of τ can the be obtained from Eq. (8) as

$$\sigma_z = \frac{1}{\Gamma_{12}}\left[\Gamma_{11}\tau_{,x} - \tau_{,xxx}\right]. \tag{17}$$

Substituting expressions of τ from Eq. (13) and σ_z from Eq. (17) in Eq. (16), we get three set of algebraic equations that need to be solved simultaneously to obtain C_i $(i = 1, 2, 3)$:

$$\boldsymbol{A}\boldsymbol{C} = \boldsymbol{F}, \tag{18}$$

where $\boldsymbol{C} = [C_1 \quad C_3 \quad C_5]^T$ and $\boldsymbol{F}$ contains:

$$F_1 = \frac{1}{\beta_1}\left(\bar{d}_{31}E_z - \frac{6\bar{\lambda}_{19}}{h_t}\bar{E}_z\right), \quad F_2 = -\frac{12\bar{\lambda}_{19}}{h_t^2\beta_2}\bar{E}_z, \quad F_3 = 0. \tag{19}$$

The matrix $\boldsymbol{A}$ in Eq. (18) is defined in [4]. Solving Eq. (18) for three constants, Eqs. (13) and (17) are used to obtain the expressions for τ and σ_z, respectively.

RESULTS AND DISCUSSION

VALIDATION

TABLE I. MATERIAL PROPERTIES.

Material	Y_1	Y_2	Y_3	G_{23}	G_{13}	G_{12}	ν_{23}	ν_{13}	ν_{12}
	(GPa)								
Gr/Ep [7]	181	10.3	10.3	2.87	7.17	7.17	0.28	0.28	0.33
PZT-5H [3]	66.67	66.67	47.62	23	23	23.5	0.51	0.51	0.29
	Y	G	ν	d_{31}	d_{32}		μ_{19}	μ_{39}	
	(GPa)			($\times 10^{-12}$mV^{-1})			(μC/m)		
BST [8,9]	150	-	0.3	-	-		8.5	100	
PZT-5H [3]	-	-	-	-265	-265		-	-	
Adhesive [3]	4.7	1.67	-	-	-	-	-	-	

Since no analytical model is currently available for actuation using physically modeled surface-bonded piezoelectric or flexoelectric transducers, we validate our developed analytical model by comparing the results with the 2D finite element (FE) solution obtained using ABAQUS. Notably, most commercial software, including ABAQUS, does not have a built-in flexoelectric constitutive model. Therefore, we physically modeled the actuator by considering piezoelectric material in the FE model. For this purpose, we consider a host laminate-adhesive-actuator system having geometrical dimensions as

$h = 1$ mm, $h_t = 0.1$ mm, $h_a = 50$ μ m, and $a = 14$ mm, unless stated otherwise. The composite host laminate consists of four graphite-epoxy (Gr/Ep) layers with a symmetric layup of $[0°/90°]_s$, with each layer having equal thickness throughout the analysis. The piezoelectric transducer is taken as lead zirconate titanate (PZT-5H). The material properties of the substrate, transducer, and adhesive are listed in Table I.

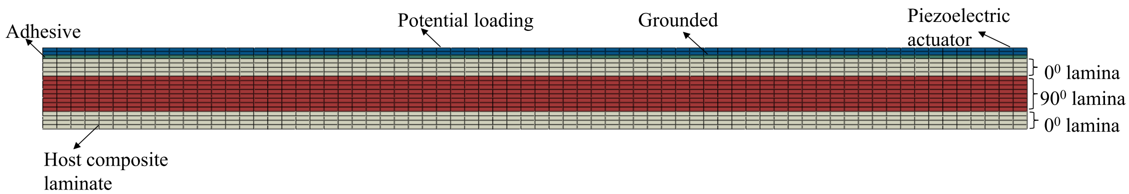

Figure 2. 2D FE model for the actuator-adhesive-host laminate system showing mesh configuration.

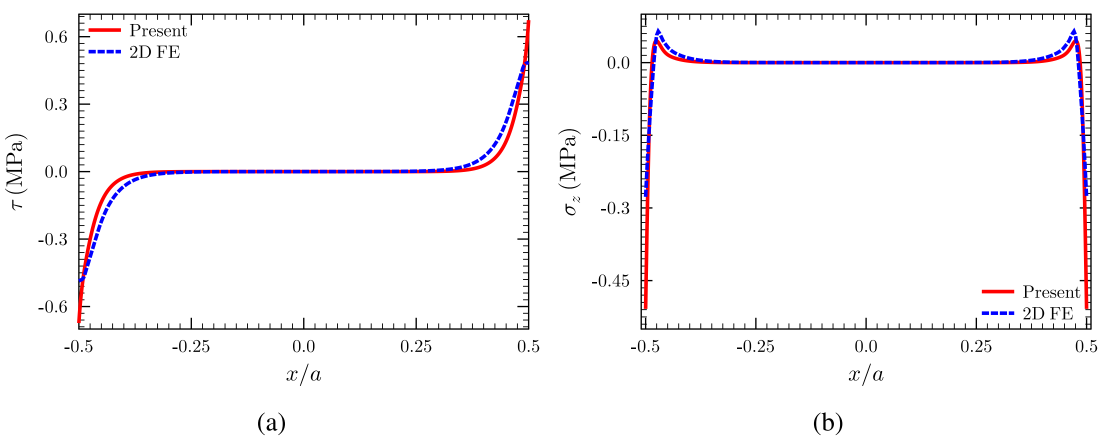

Figure 3. Comparison of present analytical solution with 2D FE model for interfacial shear and peel stress distribution.

In the FE analysis, the host plate and the adhesive are modeled using the eight-node quadrilateral element plane strain element (CPE8R) with reduced integration, while the actuator is modeled with plane strain eight-node piezoelectric quadrilateral element (CPE8E). The thickness of the actuator, adhesive, and host laminate is discretized with two, one, and sixteen elements, respectively. Along the longitudinal direction, the element length is set to 0.2 mm for the entire system. As we consider stress-free edges for the actuator and host structure, no mechanical boundary conditions are applied at either end. However, for electrical loading, a static voltage of 20 V is applied at the top surface of the actuator, while the bottom surface of the transducer is electrically grounded.

The present analytical solution for interfacial shear and peel stresses is compared with the 2D FE solution, as shown in Fig. 3. The results show a close agreement with the 2D FE solution for both shear and peel stresses, thereby validating the current model.

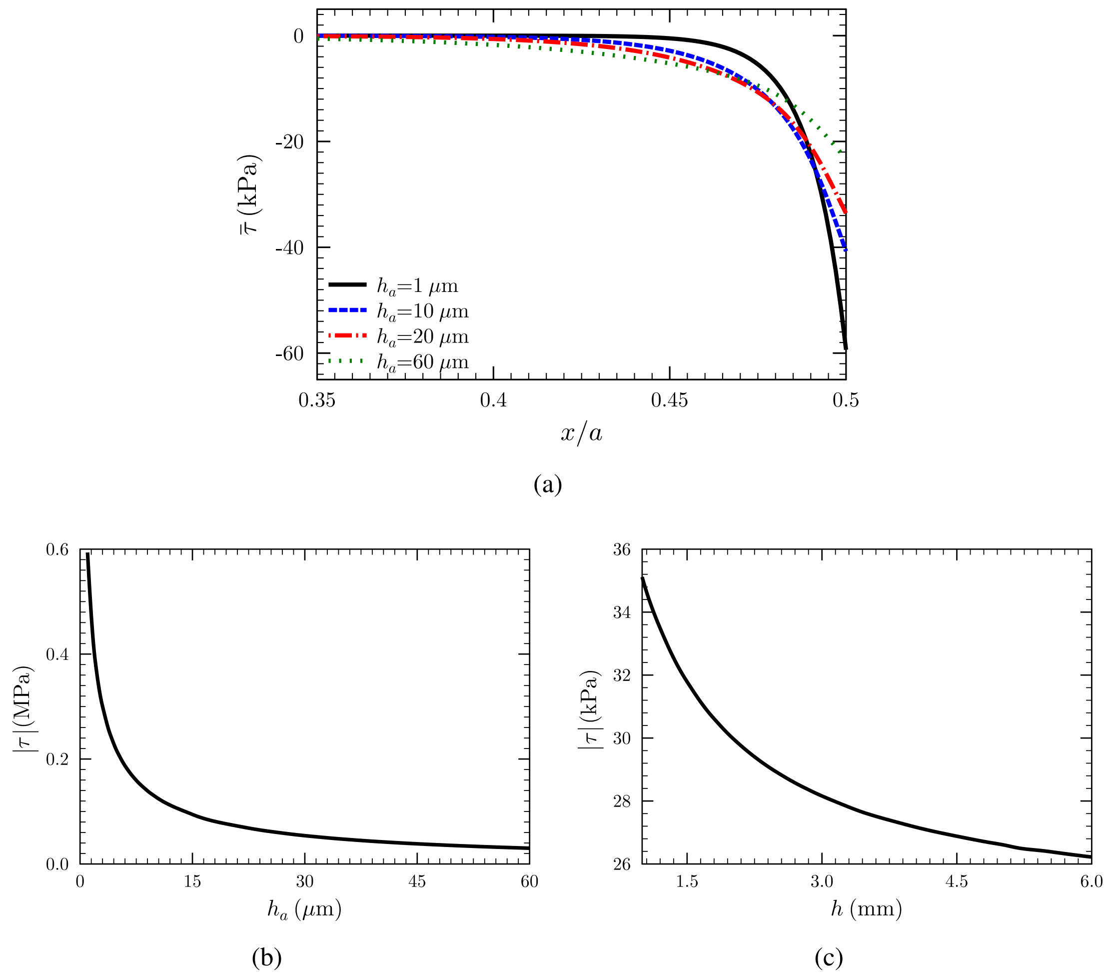

Figure 4. Effect of adhesive thickness (a) on the longitudinal distribution of $\bar{\tau} = \tau\sqrt{h_a/h_t}$ and Effect of (b) adhesive thickness and (c) host laminate thickness on the peak magnitude of shear stress.

EFFECT OF ADHESIVE AND HOST LAMINATE THICKNESS ON INTERFACIAL SHEAR STRESS

In this section, we illustrate the effect of adhesive thickness on the longitudinal distribution of interfacial shear stress. Further studies show the influence of h_a and h on the peak magnitude of interfacial shear stress. For this analysis, we consider a flexoelectric material, barium strontium titanate (BST), as the actuator.

Figure 4(a) depicts the effect of h_a on the longitudinal distribution of interfacial shear stress $\bar{\tau} = \tau\sqrt{h_a/h_t}$. As expected, peak magnitudes of $\bar{\tau}$ increase, and their distributions become more localized near the actuator edge as the adhesive becomes thinner. Further, the effect of h_a and h on the peak magnitude of τ is plotted in Figs. 4(b) and (c), respectively. It can be observed from both figures that the peak magnitude of the interfacial shear stress increases with a decrease in both h_a and h. Specifically, in Fig. 4(b), the peak magnitude of shear increases sharply below $h_a = 15$ μm and approaches a nearly constant value for $h_a \geqslant 45\ \mu$m. In contrast, Fig. 4(c) shows a nonlinear gradual increment in peak magnitude as h decreases.

CONCLUSION

For the first time, we have developed a theoretical model for actuating Lamb wave in composite plates using physically modeled adhesively bonded piezoelectric-flexoelectric transducers. The model accounts for both interfacial shear and peel stresses at the interface of the actuator and host composite laminate. To validate the model, the longitudinal distribution of interfacial shear and peel stresses are compared with the 2D FE results obtained for the piezoelectric transducer using ABAQUS.

The interfacial shear stress is more concentrated near the actuator edge, with peak value increasing as the adhesive layer becomes thinner, approaching a rigid bonding. Both a thinner adhesive layer and host laminate induce large peak magnitude interfacial shear stress. However, the increase is significantly sharp for $h_a < 15\ \mu$m and becomes almost asymptotic above $h_a = 45\ \mu$m. On the other hand, the increase in peak magnitude of interfacial shear with decreasing host laminate thickness follows a gradual nonlinear trend. The developed actuator model will be useful for obtaining analytical solution for Lamb wave excitation and propagation in composite plate using piezo-flexoelectric transducers.

REFERENCES

1. Tagantsev, A. 1985. "Theory of flexoelectric effect in crystals," *Journal of Experimental and Theoretical Physics*, 88(6):2108–22.
2. Kapuria, S. and J. K. Agrahari. 2018. "Shear-lag solution for excitation, sensing, and time reversal of Lamb waves for structural health monitoring," *Journal of Intelligent Material Systems and Structures*, 29(4):585–599.
3. Kapuria, S., B. N. Sharma, and A. Arockiarajan. 2022. "Role of transducer inertia in generation, sensing, and time-reversal process of Lamb waves in thin plates with surface-bonded piezoelectric transducers," *Journal of Intelligent Material Systems and Structures*, 33(6):779–798.
4. Rout, S. K. and S. Kapuria. 2023. "A flexoelectric actuator model with shear-lag and peel stress effects," *Proceedings of the Royal Society A: Mathematical, Physical and Engineering Sciences*, 479(2273):20230099.
5. Jain, M., S. Kapuria, and S. Pradyumna. 2022. "Efficient time-domain spectral element with zigzag kinematics for multilayered strips," *International Journal of Mechanical Sciences*, 232:107603.
6. Smirnov, V. I. 1964. *A course of higher mathematics: Elementary calculus*, vol. 1, Pergamon Press; [U.S.A. ed. distributed by Addison-Wesley Publishing Company, Reading, Mass.
7. Ahmed, A. and S. Kapuria. 2017. "Third order theory based quadrilateral element for delaminated composite plates with a hybrid method for satisfying continuity at delamination fronts," *Composite Structures*, 181:84–95.
8. Wei, C., Z. Wang, and W. Huang. 2021. "Performance of a flexoelectric actuator for Lamb wave excitation," *Journal of Applied Physics*, 129(3):034902.
9. Sharma, S., R. Kumar, and R. Vaish. 2021. "Universal converse flexoelectricity in dielectric materials via varying electric field direction," *International Journal of Smart and Nano Materials*, 12(1):107–128.